An Extension of the Swarmalator Model

Ankith Anil Das

Synchronization occurs at many natural and technological systems. Such an emergent properties is observed in cardiac pacemaker cells, Japanese tree frogs, colloidal suspensions of magnetic particles, and other biological and technological systems in which synchronization interact. We consider a system where phase dynamics and spacial dynamics are coupled. A detailed analysis of such a system was proposed by Kevin P. O'Keeffe in the paper . We studied an extension of the Swarmalator model proposed in the paper. Understanding the dynamics of this model could possibly give insight to the generalized model where the phase coupling function could be a fourier series.

I. Introduction

Synchronization in oscillations occurs in many natural systems, including the activity of the brain[1], and synchronous firefly flashing[2], as well as many engineering applications, such as power grids[3], and Josephson junction arrays[4]. Kuramoto model [5] was one of the first major analysis in synchronization of coupled oscillators. Kuramoto's discovery of critical coupling strength, above which causes spontaneous synchronization was a breakthrough in the dynamics of coupled oscillators. This model has been generalized to other large systems of biological oscillators, such as chorusing frogs[6], firing neurons[7], and even human concert audiences clapping in unison[8].

One area which has come under recent light is the collective study of swarming and synchronization. Both synchronization and swarming involve large,self organizing groups which interact according to some set of simple rules. Studies involving swarming of animals focus on spacial dynamics, while ignoring internal state. On the other hand, studies involving synchronization focus on phase dynamics and not their motion. A combined model was proposed by O'Keeffe et al. [9], which looked into the collective dynamics of phase and position of oscillators. He called such oscillators "swarmalators" to highlight their dual nature. In this mini report, we will be looking into an extended model which has a more general phase coupling function. Our motivation for such an extension was to understand the behavioral changes of system, whose results could help us generalize the phase coupling function to a fourier sin series.

II. The Model

We consider swarmalators free to move in the plane. The governing equations are [9]

$$\dot{\mathbf{x}}_i = \mathbf{v}_i + \frac{1}{N}\sum_{j=1}^{N}\left[\mathbf{I}_{\text{att}}\left(\mathbf{x}_j - \mathbf{x}_i\right) F\left(\theta_j - \theta_i\right) - \mathbf{I}_{\text{rep}}\left(\mathbf{x}_j - \mathbf{x}_i\right)\right] \tag{1}$$

$$\dot{\theta}_i = \omega_i + \frac{K}{N}\sum_{j=1}^{N} H_{\text{att}}\left(\theta_j - \theta_i\right) G\left(\mathbf{x}_j - \mathbf{x}_i\right) \tag{2}$$

for $i = 1, \ldots, N$, where N is the number of swarmalators, $\mathbf{x}_i$ is the position of the i-th swarmalator, and θ_i, ω_i, and $\mathbf{v}_i$ are it's phase, natural frequency and background velocity. The functions $\mathbf{I}_{att}$ and $\mathbf{I}_{rep}$ represent spatial attraction and repulsion between the swarmalators where as phase interaction is governed by $\mathbf{H}_{att}$. We considered the following model:

$$\dot{\mathbf{x}}_i = \mathbf{v}_i + \frac{1}{N}\left[\sum_{j\neq i}^{N}\frac{\mathbf{x}_j - \mathbf{x}_i}{|\mathbf{x}_j - \mathbf{x}_i|}\left(1 + J\cos\left(\theta_j - \theta_i\right)\right) - \frac{\mathbf{x}_j - \mathbf{x}_i}{|\mathbf{x}_j - \mathbf{x}_i|^2}\right] \tag{3}$$

$$\dot{\theta}_i = \omega_i + \frac{K}{N}\sum_{j\neq i}^{N}\frac{\gamma_1 \sin\left(\theta_j - \theta_i\right) + \gamma_2 \sin\left(2\left(\theta_j - \theta_i\right)\right)}{|\mathbf{x}_j - \mathbf{x}_i|} \tag{4}$$

We considered identical swarmalators so that $\omega_i = \omega$ and $\mathbf{v}_i = \mathbf{v}$. Using this assumption, using a suitable choice of reference frame we can set $\omega = 0$, and $\mathbf{v} = \mathbf{0}$. The system has four parameters $(J, K, \gamma_1, \gamma_2)$.

The parameter J measures the extend to which phase similarity enhances spatial attraction. For $J > 0$, swarmalators prefer to be near other swarmalators with similar phase. When $J < 0$, the opposite behavior is observed: swarmalators attract those with opposite phase. When $J = 0$, they show no phase based spatial behavior,i.e, their spatial attraction is independent of phase. To maintain $\mathbf{I}_{att} > 0$, we constrain J to $-1 \leq J \leq 1$. The parameter K is the phase coupling strength which scales γ_1, and γ_2. The relative strengths of γ_1 and γ_2 determine the stability of one or two clusters.

Before stating the dynamics of the system, we pause to state the features of this model. This model's purpose is to study the interplay between swarming and synchronization. Our model accounts for aggregation, but not alignment. There are no alignment terms. We chose to neglect orientation because it adds another layer of complexity; it makes each swarmalator have four state variables. For rest of the report we will refer to our model as 'Dual phase coupled model' because of the presence of double angle sin function in Eq.4. In a similar fashion, the original model proposed by P. O'Keeffe will be referred as 'Single phase coupled model'.

III. Optimization of the ode solver

The simulations were run using MATLAB's ODE integrator 'ode45'. Absolute and Relative tolerance for the integrator was set to 10^{-6}. Before large computations

were performed, optimisation of the existing code was necessary. As this project involves computations of large matrices using ode45, optimising the code for speed was essential for any extensive calculation. The initial code was profiled using MATLAB's performance profiler, and bottlenecks were identified. Calculating the pairwise inverse distance was the most computationally expensive part in the ode function. The original code took 70 seconds for a simulation with $N = 100$ and $T = 10$-time units. This speed was too slow for any extended time simulations. After removing unwanted function calls, changing the algorithm, and using functions which supports vectorization, the new code took 0.509 sec for the same task. The performance was good enough for an interactive user simulation where the user can change the parameters of the system and can see the results almost instantly.

IV. Cluster formation and stability

The dynamics of dual phase coupled model had some striking differences with the original single phase model. The system not only settled in all the five states which were discussed in detail by Kevin P. O'Keeffe in single phase model, but also showed many additional stable and metastable states. Understanding the behavior of the modified phase coupling term and how it affects the formation of states could give us deep insights about the generalization of the model. The additional cluster states made by the model can be broadly classified as follows

(a) Static two cluster state

(b) Static bimodal single cluster state.

(c) Two cluster state with rogues

(d) Active three-four cluster state

(e) Active single cluster state

To understand system behavior under the change of γ_1, and γ_2, we chose $J = 0.8$ and $K = -0.5$ which represent Active phase wave in single phase coupled model. This set of state variables were chosen because it showed the most active spacial behavior in single phase coupled model and the dynamics of the system would be more depended on the values of γ_1 and γ_2. Unless otherwise stated, the simulations are run with $J = 0.8$ and $K = -0.5$. Also, all the simulations were run with random initial position in a 1x1 box and phases from $[-\pi, \pi]$, both uniformly and random. To maintain consistency, the same random seed was used for all simulations.

V. Static Two cluster state

Static two cluster case is a very common equilibrium state seen for various values of $(J, K, \gamma_1, \gamma_2)$, illustrated in Fig.1. Since $J > 0$, 'like attracts like': swarmalators want to settle near other swarmalators with similar phase. Looking at phase dynamics equation (Eq.4) $\dot{\theta}_i = 0$ when $\theta_i = C, C + \pi$, where C is any constant.

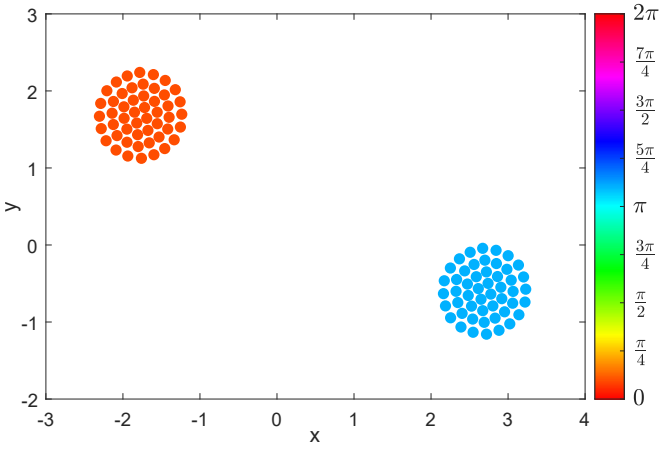

FIG. 1. Static two Cluster State. This state was achieved for $N = 100$, $\gamma_1 = 2/3$, and $\gamma_2 = -0.5$. The simulation was run for $T = 100$ time steps with variable step-size (ode45) for the system to settle down.

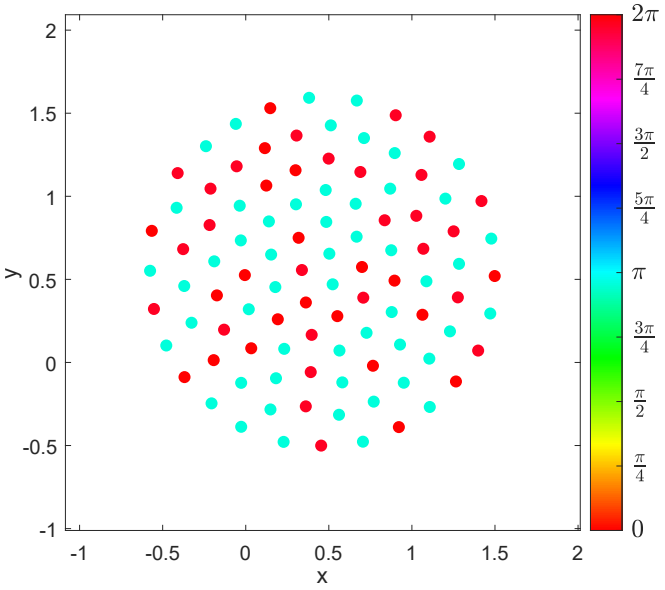

FIG. 2. Static bimodal single cluster state. This state was achieved for $N = 100, K = -0.5, J = -0.8, \gamma_1 = 2/3, \gamma_2 = -0.1$ after $T = 300$ time steps.

Due to the presence of a new stable phase, the system can form two clusters with π phase difference. Now for the given value of K which is less than 0, $\gamma_1 > 0$ (Negative coupling) implies the system does not prefer single cluster state, and $\gamma_2 < 0$ (positive coupling) means the system prefers to stabilize in two cluster state. Furthermore, $|\gamma_2| > |\gamma_1|$ shows that the second coupling term in Eq.4 is more dominant in stabilizing the system. Fig.6 shows how the phase settles with time. Here, the phase effectively stabilizes to two values after taking mod 2π. The average cluster phase difference is approximately π with an absolute error $\epsilon \approx 2.6074 \times 10^{-9}$. Our statement about two cluster phase difference therefore agrees with

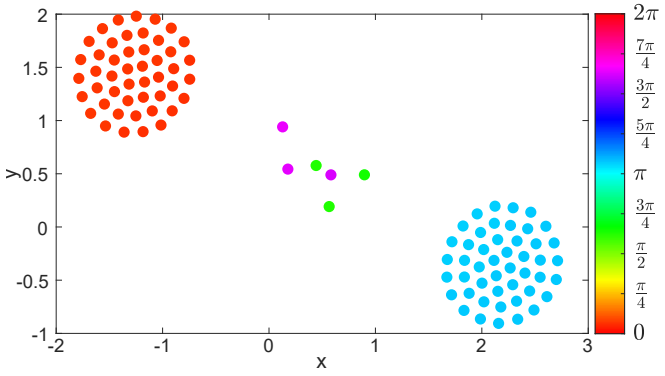

FIG. 3. Two Clusters with Rogues. This state was reach under a random run with $\gamma_1 = 2/3, \gamma_2 = -1/3$ after $T = 200$ time steps.

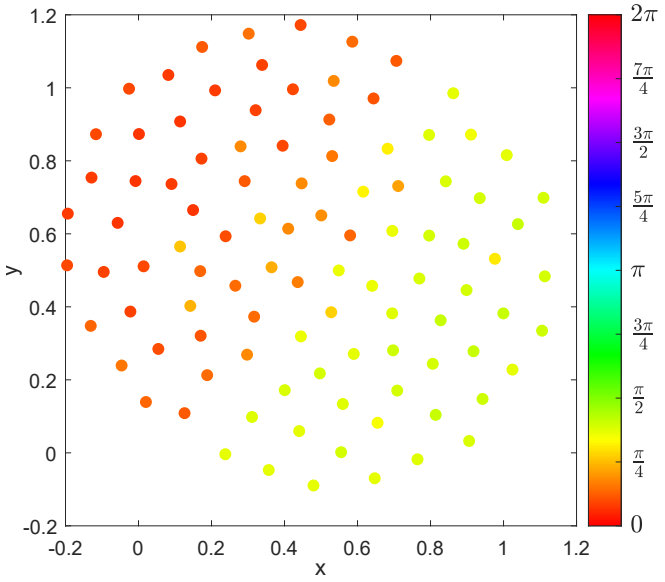

FIG. 4. Active Single cluster state.This state was achieved for $N = 100$, $\gamma_1 = -1$, and $\gamma_2 = +0.72$. It is a non-stationary state where swarmalators on the boundary of the two phase clusters jump from one side of the cluster to other.

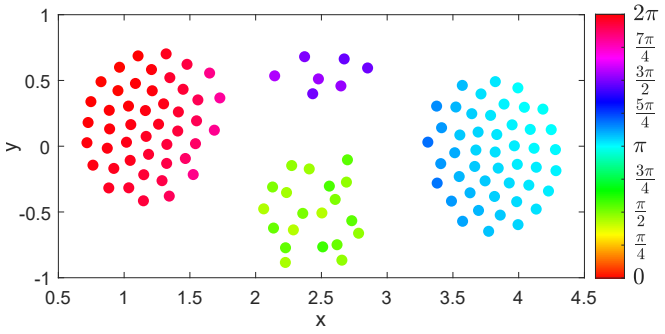

FIG. 5. Active 4 cluster state. This special state was achieved by manually adding 20 swarmalators of phase $\pi/2$ in the middle of two clusters with phase 0 and π. The figure shows the state after $T = 300$ time steps

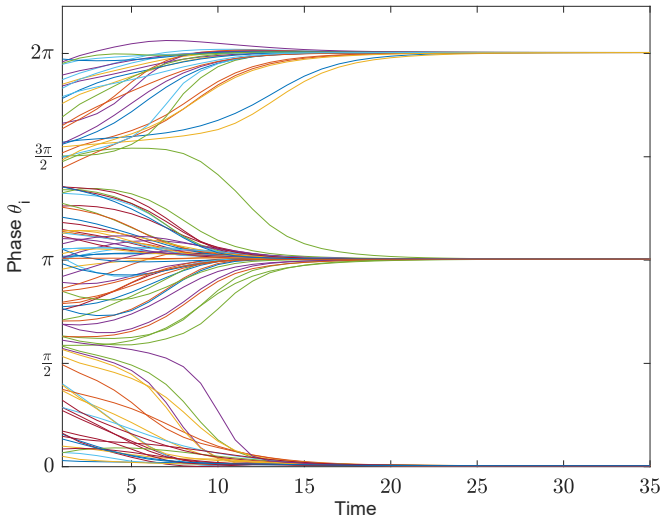

FIG. 6. Phase of the Swarmalator vs Time.

the simulations.

A. Inter-cluster distance for Static two cluster state

We can analytically solve the inter-cluster distance for static two cluster state by making an assumption. Let,

$$\mathbf{C}_0 = \frac{1}{N_0}\sum_{i\in S_0}\mathbf{x}_i \quad \text{and} \quad \mathbf{C}_\pi = \frac{1}{N_\pi}\sum_{i\in S_\pi}\mathbf{x}_i, \tag{5}$$

where $\mathbf{C}_0$ and $\mathbf{C}_\pi$ are the centroids of the clusters with average phase approximately equal to 0 and π respectively , and S_0 and S_π are the respective clusters. Differentiating $\mathbf{C}_0$ w.r.t time gives

$$\begin{aligned}
&N_0\dot{\mathbf{C}}_0 \\
&= \sum_{i\in S_0}\dot{\mathbf{x}}_i \\
&= \sum_{i\in S_0}\sum_{j=1}^{N}\left(\frac{\mathbf{x}_j-\mathbf{x}_i}{|\mathbf{x}_j-\mathbf{x}_i|}\left(1+J\cos(\theta_j-\theta_i)\right)-\frac{\mathbf{x}_j-\mathbf{x}_i}{|\mathbf{x}_j-\mathbf{x}_i|^2}\right) \\
&= \sum_{i\in S_0}\Bigg(\underbrace{\sum_{j\in S_0}\left(\frac{\mathbf{x}_j-\mathbf{x}_i}{|\mathbf{x}_j-\mathbf{x}_i|}(1+J)-\frac{\mathbf{x}_j-\mathbf{x}_i}{|\mathbf{x}_j-\mathbf{x}_i|^2}\right)}_{=0,\text{since pair wise cancellation}}+ \\
&\sum_{j\in S_\pi}\left(\frac{\mathbf{x}_j-\mathbf{x}_i}{|\mathbf{x}_j-\mathbf{x}_i|}(1+J)-\frac{\mathbf{x}_j-\mathbf{x}_i}{|\mathbf{x}_j-\mathbf{x}_i|^2}\right)\Bigg) \\
&= \sum_{i\in S_0}\sum_{j\in S_\pi}\frac{\mathbf{x}_j-\mathbf{x}_i}{|\mathbf{x}_j-\mathbf{x}_i|^2}\left((1+J)|\mathbf{x}_j-\mathbf{x}_i|-1\right)
\end{aligned}$$

We will make the assumption that $|\mathbf{x}_j - \mathbf{x}_i| \approx |\mathbf{C}_0 - \mathbf{C}_\pi| = r$ (say). Then

$$N_0 \dot{\mathbf{C}}_0 \approx \sum_{i \in S_0} \sum_{j \in S_\pi} \frac{\mathbf{x}_j - \mathbf{x}_i}{r^2} \left((1+J)r - 1\right)$$

$$= \frac{(1+J)r-1}{r^2} \left(\sum_{i \in S_0} \sum_{j \in S_\pi} \mathbf{x}_j - \mathbf{x}_i \right)$$

$$\dot{\mathbf{C}}_0 = N_\pi \frac{(1+J)r-1}{r^2} (\mathbf{C}_\pi - \mathbf{C}_0). \tag{6}$$

Using similar arguments we can also find $\dot{\mathbf{C}}_\pi$,

$$\dot{\mathbf{C}}_\pi = N_0 \frac{(1+J)r-1}{r^2} (\mathbf{C}_0 - \mathbf{C}_\pi). \tag{7}$$

Finally,

$$\dot{\mathbf{C}}_0 - \dot{\mathbf{C}}_\pi = -N \left(\frac{(1-J)r-1}{r^2} \right) (\mathbf{C}_0 - \mathbf{C}_\pi)$$

$$\Rightarrow \frac{dr}{dt} = -N \left(\frac{(1-J)r-1}{r} \right). \tag{8}$$

Equating Eq.8 to zero gives the equilibrium distance between the cluster,

$$r^* = \frac{1}{1-J} \tag{9}$$

Surprisingly but yet obvious, the inter-cluster distance is independent of N, K, γ_1,and γ_2. To verify our analytical solution, simulations were run for various values of N and K and the results are shown in Fig.7 and Fig.8. These figures shows agreement between these predictions and simulations. Also, from Eq.9, we realize that for $J > 1$ the two clusters move to infinity.

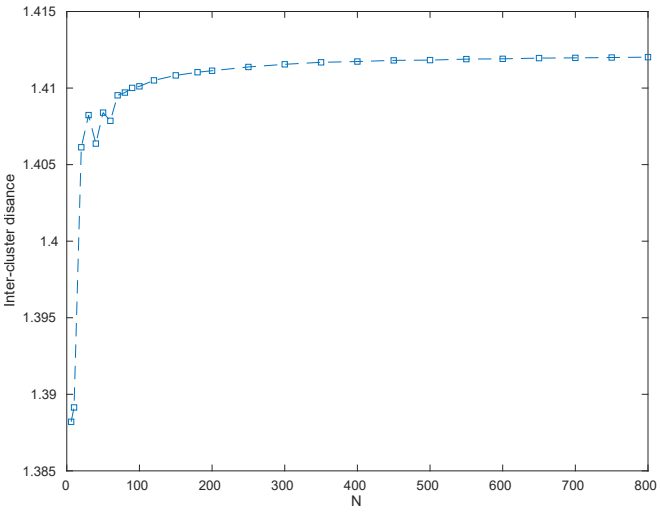

FIG. 7. Inter-cluster distance for static two cluster state. Simulations were run for various values of N with $K = -0.5, J = 0.3, \gamma_1 = 2/3, \gamma_1 = -1/3$. Swarmalators were initially positioned in two equally sized clusters with average phase 0 and π and simulations were run for $T = 300$ time steps.

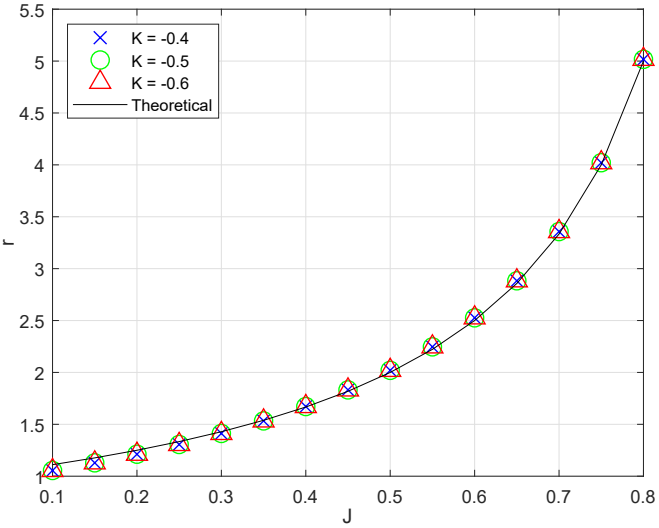

FIG. 8. Inter-cluster distance for varying K. Simulations were run for various values of K and J for $N = 800$. The black line shows the theoretical prediction as per Eq.9. The figure justifies that inter-cluster distance is independent of K.

VI. Two clusters with Rogues

Two clusters with rouges is a special non-stationary state which occurs for values of γ_1 and γ_2 "close" to $2/3$ and $-1/3$ respectively. From our analysis we couldn't conclusively find the exact region where this state was possible. We encountered this state mostly when we ran random simulations with $\gamma_1 = 2/3$ and $\gamma_2 = -1/3$. We also tried adding swarmalators in the middle of static two cluster state to understand how γ_1 and γ_2 influenced the formation of rogues, but we weren't able to get conclusive results. Looking into the dynamics, the presence of rogues caused the clusters to come closer and execute oscillations as the rogues moved back and forth. The system settled down to a stationary state only for the case with one rogue swarmalator. The rogues would always form clusters with similar phase which would pass through each other while moving back and forth. These spacial oscillations causes phase oscillations of the rogues and the clusters. Fig.9 shows the phase oscillations of the rogues and clusters. After running the simulation for $N = 100$ case for $T = 1000$ time steps, the first half of which were discarded, the phase was averaged for each cluster. The two big cluster had a phase difference of approximately π and the rogues had a phase difference of approximately $\pi/2$ from the clusters.

VII. Active single cluster state

Active single cluster state is a special single cluster state when $-\gamma_1 < 2\gamma_2$ where $\gamma_1 < 0$. Due to γ_1 being negative, the system prefers to be in a single cluster state, but at the same time, positive γ_2 makes the system split into two phase clusters. Such opposite behavior of γ_1 and γ_2 makes the system reach such a state. Swarmalators along the boundary of phase clusters jump from one cluster to another. Even after running the simulations

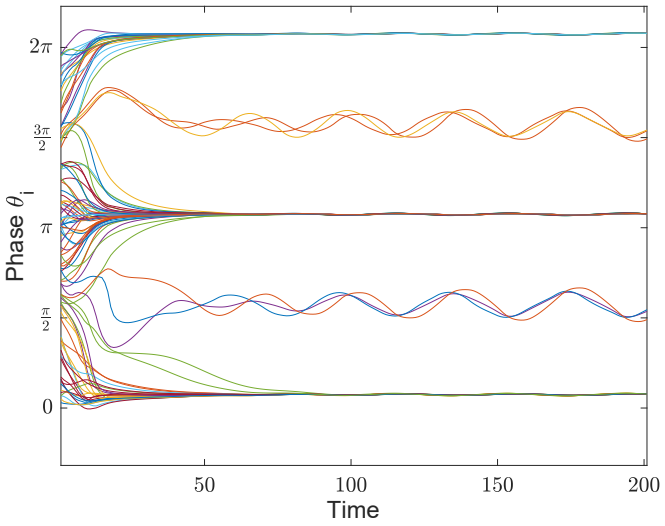

FIG. 9. Phase of Swarmalator Vs Time for two clusters with rogues. The figure shows rogues performing sinusoidal phase oscillations with mean phase $\pi/2$ off from the big clusters. Simulations were run for $N = 100$ for 200 time steps with $\gamma_1 = 2/3$ and $\gamma_2 = -1/3$.

for a long time ($T > 2000$), the system didn't show signs of settling down. Fig. 4 shows how the phase is split between the clusters.

VIII. Active three-four cluster state

Active three-four cluster state is a special extension of two cluster with rogues state. Under random runs such a state was never achieved. The state shown in Fig. 5 was created by placing 20 swarmalators of phase $\pi/2$ in the middle of two clusters with phase 0 and π. The two big clusters are brought together much closer than any other states and there is a smooth gradient of phase within the cluster. The clusters in the center perform random motion within the cluster while the boundary swarmalators of the big clusters perform circular motion. There is no longer back and forth motion of the center clusters. Such a state is also possible with three clusters.

IX. Static bimodal single cluster state

This state is reached when $J < 0$ with $K > 0, \gamma_1 < 0$, and $\gamma_2 > 0$ or $K < 0, \gamma_1 > 0$, and $\gamma_2 < 0$. If sign of γ_2 is flipped, the state changes to static async. Here the phase difference between the swarmalators is very close to π. A similar state is achieved for $J = 0$, which is expected since Eq.3 is phase decoupled.

X. Stability

In this section we will briefly look into the stability of the above states. We will focus our analysis into phase stability since stable phase dynamics consequently implies stable spacial dynamics.

Calculating the jacobian is fairly straightforward for Eq.4.

$$\mathbf{J} = \left(\frac{\partial \theta_i}{\partial \theta_j}\right) = \frac{K}{N}\begin{cases} -\sum_{k\neq i} \frac{\gamma_1 \cos(\theta_k-\theta_i)+2\gamma_2\cos(2(\theta_k-\theta_i))}{|\mathbf{x}_k-\mathbf{x}_i|} & i=j \\ \frac{\gamma_1\cos(\theta_j-\theta_i)+2\gamma_2\cos(2(\theta_j-\theta_i))}{|\mathbf{x}_j-\mathbf{x}_i|} & i\neq j \end{cases} \tag{10}$$

First point of interest in this matrix $\mathbf{J1} = \mathbf{0}$. Therefore 0 is an eigenvalue. This result was not surprising as we already know that shifting the phase by a constant value does not change the dynamics of the system.

For Single cluster case, $\theta_i = 0$.

$$\begin{aligned} \mathbf{J}|_{\theta_i=0} &= \frac{K}{N}\begin{cases} -\sum_k A_{ik}(\gamma_1+2\gamma_2) & i=j \\ A_{ij}(\gamma_1+2\gamma_2) & i\neq j \end{cases} \\ &= -\frac{K}{N}(\gamma_1+2\gamma_2)\begin{cases} \sum_k A_{ik} & i=j \\ -A_{ij} & i\neq j \end{cases} \\ &= -\frac{K}{N}(\gamma_1+2\gamma_2)\mathbf{M} \end{aligned} \tag{11}$$

where $A_{ij} = |\mathbf{x}_j - \mathbf{x}_i|^{-1}$ with $A_{ii} = 0$. Here $\mathbf{M}$ is a weighted Laplacian matrix and therefore semi-positive definite. Therefore the eigenvalues of J are

$$\mathbf{J}: \begin{cases} \lambda_i \geq 0 & \text{if } -K(\gamma_1+2\gamma_2) > 0 \\ \lambda_i = 0 & \text{if } -K(\gamma_1+2\gamma_2) = 0 \\ \lambda_i \leq 0 & \text{if } -K(\gamma_1+2\gamma_2) < 0 \end{cases} \tag{12}$$

This result gives us deep insight about single cluster stability. For a fixed value of $K < 0$, single cluster state is only stable when $\gamma_1 + 2\gamma_2 < 0$. For any other values of γ_1, γ_2, the system will eventually break into two clusters. Stability of single cluster for all the three cases is shown in Fig.10,11,12.

For two cluster case, we couldn't arrive at a similar analytical solution like the single cluster case. Nevertheless, we numerically calculated the eigenvalues of phase jacobian matrix to understand the stability of this state. We constructed two clusters with phase 0 and π respectively, and ran the simulation for $\gamma_1 = 2/3$, $\gamma_2 = -1/3$ for $T = 2000$ time steps for the system to reach equilibrium. Then we added perturbed phase by adding small random numbers of order 10^{-8}. We changed the values of γ_1,γ_2, ran the simulation for $T = 2000$ time steps and calculated the phase jacobian matrix at end time step. We found that for $\gamma_1 + 2\gamma_2 \leq 0$, the system was unconditionally stable, i.e, all eigenvalues of phase jacobian matrix was ≤ 0. When $\gamma_1 + 2\gamma_2 \geq 0.09$, the phase jacobian matrix had positive eigenvalues and the system eventually destabilized into active phase wave.

For static bimodal single cluster state, the phase jacobian matrix had negative eigenvalues, implying the state is in-fact static and stable. Adding small perturbation to this state always stabilized to a new equilibrium.

Finally, we looked into the eigenvalues of active states, and as expected, they had positive eigenvalues.

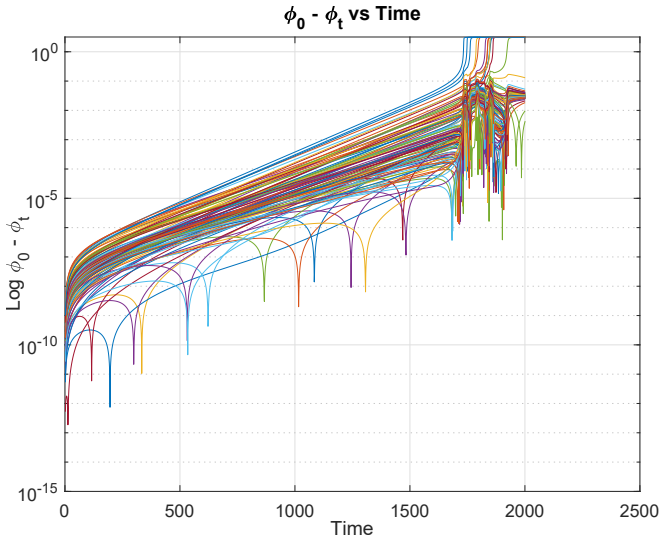

FIG. 10. Unstable single cluster case 1. In this case $\gamma_1 + 2\gamma_2 = 0.005 > 0$. From the figure, we can see that small phase perturbation of order 10^{-8} grow exponentially until the system breaks into two clusters.

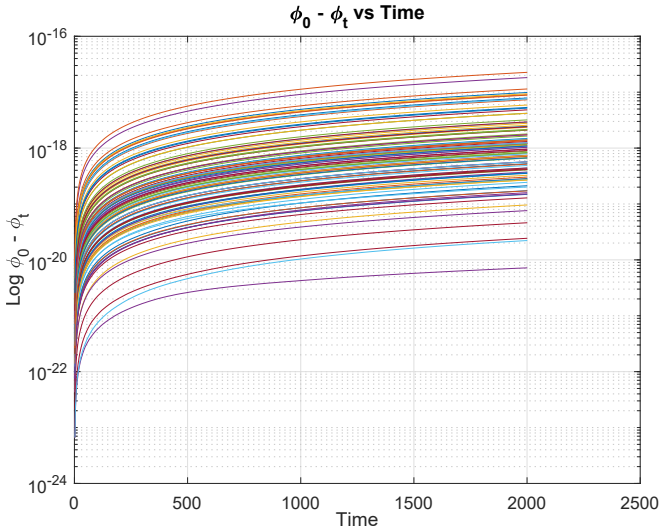

FIG. 11. Unstable single cluster case 2. In this case $\gamma_1+2\gamma_2 = 0$. Here small phase perturbation of order 10^{-8} grow linearly. Due to linear growth, it will take a significantly large amount of time for the system to break into two clusters.

XI. Periodic motion of Rogues

In this section, we will briefly look into periodic motion of rogues in two cluster with 3-3 rogues as shown in Fig. 3. Due to the static nature of the two big clusters and a small number of rogues, we expected the rogues to show periodic cyclic motion. To test this argument, we ran the simulation for 4000 time steps, the first half of which was discarded, and plotted the motion of the rogues to check if they formed closed loops. They did form closed loops as shown in Fig. 13, but there weren't completely symmetric. Such closed loops were not found when there

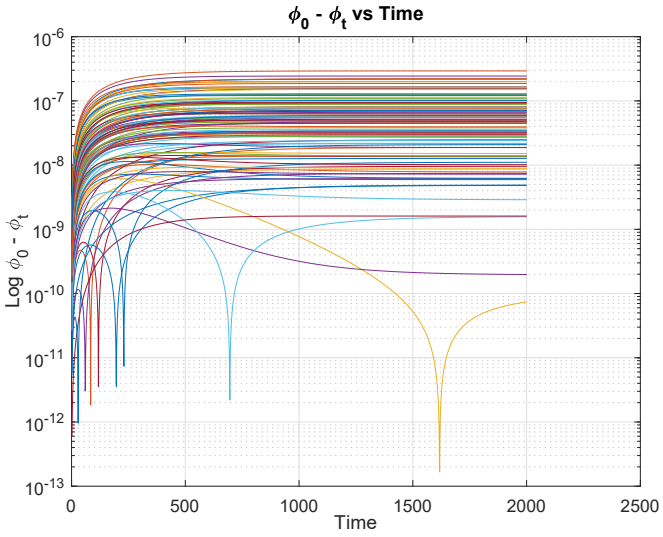

FIG. 12. Stable single cluster case 3. Here small phase perturbation of order 10^{-8} show no growth after 1700 time steps. This shows that the system has attained a new equilibrium.

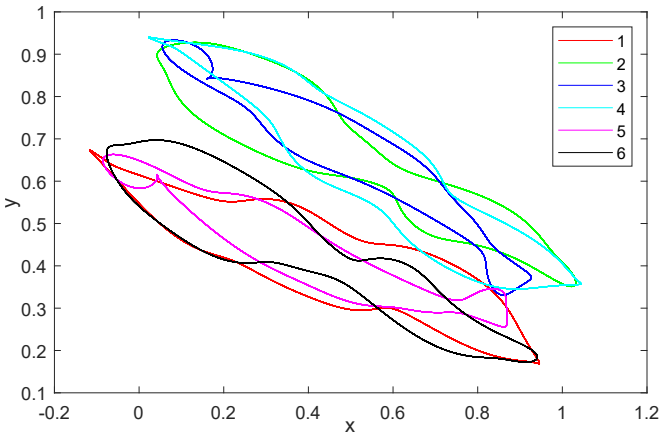

FIG. 13. Periodic motion of 3-3 rogues in two clusters with rogues state. Here particle 1,2,and 3 form one rogue cluster and the rest form another rogue cluster.

were large number of rogues. This suggest that there is a threshold over which chaos is observed in the dynamics of rogues.

XII. Circular ring state

In a search for more stable states, we encountered a special unstable equilibrium state which could be achieved by careful arrangement of swarmalators. It is achieved by placing swarmalators around a circle of half unit radius with a single swarmalator in the center. The circumferential and central swarmalators have a phase difference of π. The arrangement of swarmalators is shown in Fig. 14. Initially, the system collapses to a stable radius and maintains approximately the same radius for some time. After a critical time, the system destabilizes into two clusters. This result is shown in Fig. 15. We also looked at the distance between the centroid of the

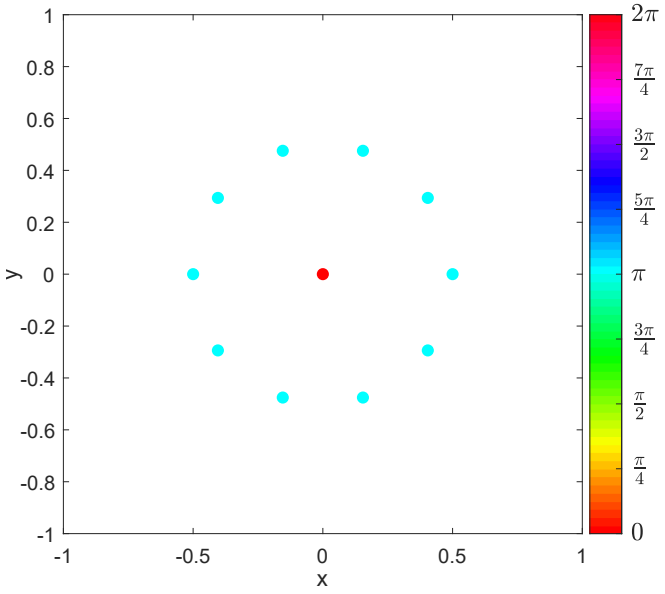

FIG. 14. Circular arrangement of swarmalators. Here the central swarmalator has phase 0 and the circumferential swarmalators have a phase π. The system has $N = 11$ swarmalators with $\gamma_1 = 2/3, \gamma_1 = -1/3$

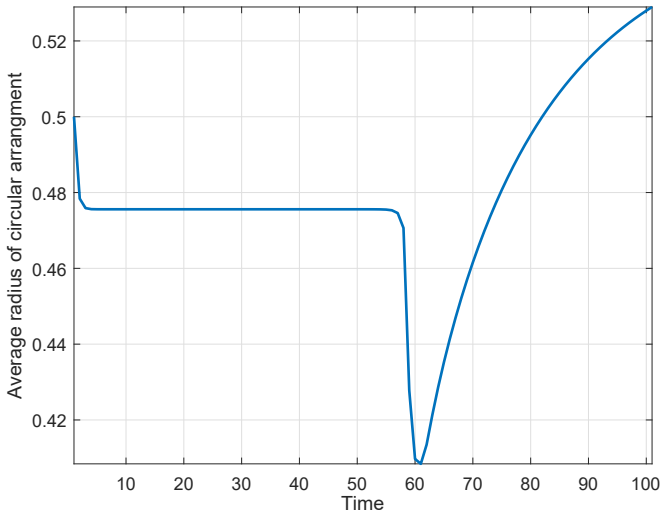

FIG. 15. Average distance of the swarmalators from the center. The circumferential swarmalators collapse to a stable radius and after a while it destabilizes into two clusters.

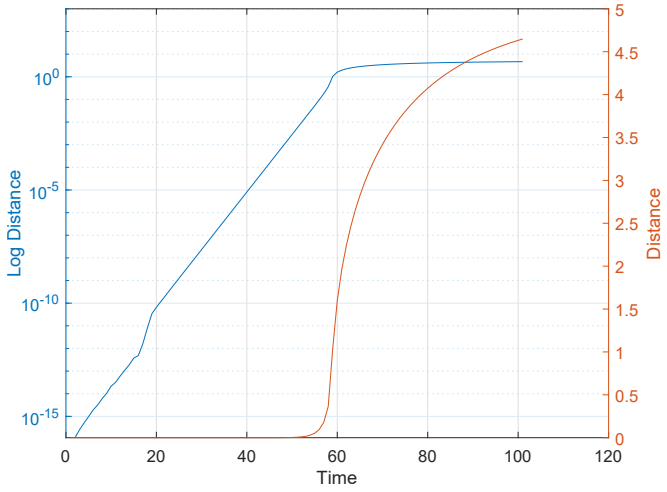

FIG. 16. Distance between the centroid of circumferential swarmalators and center swarmalator. We can see that a small perturbation of order 10^{-16} builds up exponentially until the system destabilizes into two clusters

circumferential swarmalators and the center swarmalator. From Fig. 16, we realized that a small perturbation in the arrangement of swarmalators grows exponentially until the system destabilizes into two clusters. To check if this destabilization was due to the numerical solver, we changed the absolute and relative error tolerance to 10^{-10} and this resulted in a slight increase in stable time. Further decrease in error order did not increase the stable time of the system. We also ran the simulation in single precision mode by adding an error term of order 10^{-8} to the solver function. This change to single precision decreased the stable time by half as shown in Fig.17. These tests does not confirm the numerical instability of the ode solver, but it does give insight into the sensitivity of such configuration.

XIII. Phase Variation within the clusters

So far, we have explored the collective behaviour of swarmalator in forming clusters. In this section, we will briefly talk about the behaviour of swarmalators within the cluster formation. For static two cluster case, there was little to no phase variation within the cluster. The calculated standard deviation of phase within the cluster was 2.678×10^{-17}, which for all numerical purpose is effectively zero. This is indeed quite surprising as we expected a phase gradient within the cluster due to the presence of the other cluster. Finally, adding random phase variations within the cluster led the cluster to stabilize to a different constant uniform value throughout the cluster. The average phase difference between the cluster was still approximately π.

Static bimodal single cluster is a special case where $J = 0$. The single cluster behaviour was expected as the system is effectively phase decoupled, i.e, Eq.3 has no phase term. This results in a single cluster lattice structure where the phase stabilizes to either 0 or π. Fig.2 shows the structure after the system settles.

Finally, we looked into two cluster state with rogues. To amplify the phase variations within the cluster, we ran the simulations for $N = 400$. After the system settled into two clusters with rogues in the middle, the clusters show oscillatory phase distribution within the cluster, as shown in Fig.18. There was a smooth gradient in phase, and the two clusters showed opposite phase distribution as the rogues moved back and forth.

XIV. Front end application

To showcase the dynamics of the model in a user

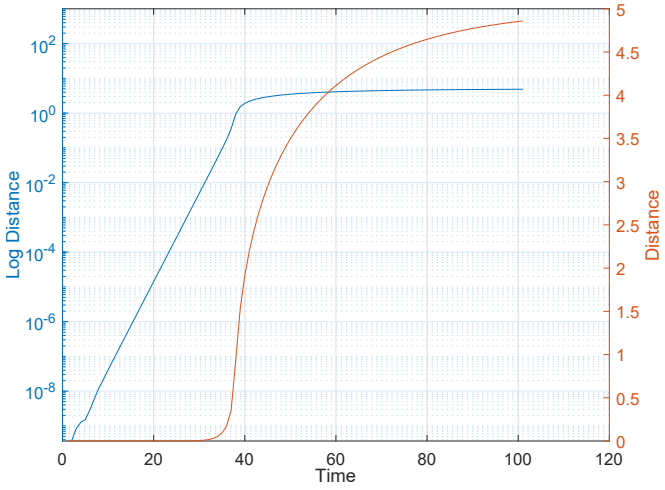

FIG. 17. Distance between the centroid of circumferential swarmalators and center swarmalator run at single precision mode. Single precision mode was simulated by adding random numbers of order 10^{-8} to the solver function. Comparing with Fig.16, the stable time has been almost reduced by half.

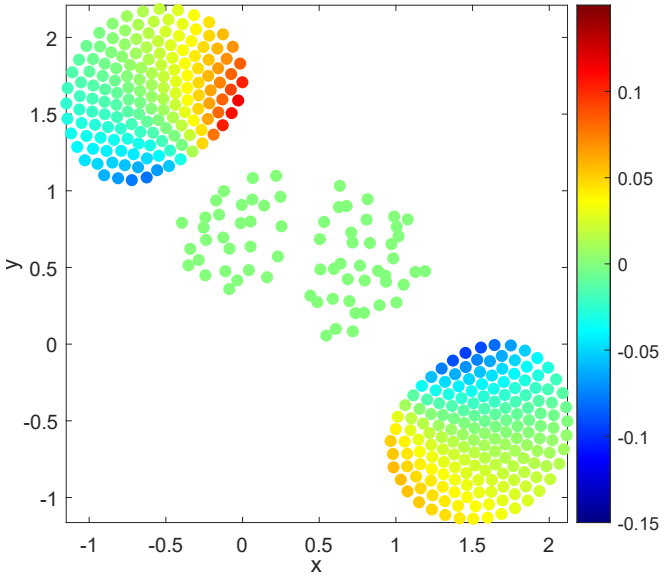

FIG. 18. Phase variation within the cluster. This simulation was run for $N = 400$ with $\gamma_1 = 2/3, \gamma_1 = -1/3$. The phase of each cluster was centered to zero by using the average phase of the cluster. The color gradient shows the variation of phase within the cluster. The phase of all rouges (center swarmalators) was set to zero for better visualization.

friendly manner, we made a GUI which displays the simulation while the model is being solved in the background. MATLAB App Designer was used to make the GUI because of its ease of use and user friendly interface. We implemented callback functions which would dynamically change model parameters and these changes can be almost seen instantaneously. We made our own ODE-plotter function which would plot output as it is being calculated by ode45. It would terminate when any

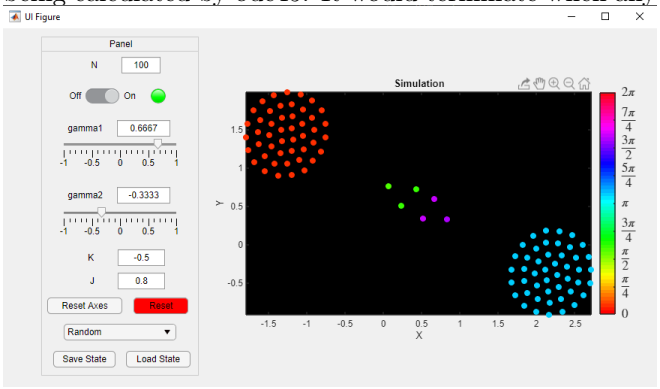

FIG. 19. GUI interface.

of the callback functions are executed, change the model parameters, and continue integration. For reasons which are unknown, implementing the model in GUI slowed down integration considerably. Even then, the animation was fast enough to show how the system responded for different parameters.

XV. Discussion

We have investigated the collective dynamics of the extended swarmalator model. These are mobile particles which have both phase and spatial degrees freedom. Furthermore, their phase and spatial dynamics are coupled. In the original single phase model, there were rich spatiotemporal patters, but they were constrained to a single cluster unit. The extended model not only showed all the states in the single phase model, but showed a variety of new states. We performed some basic analysis on these states numerically and analytically. As γ_1, γ_2 could represent the fourier coefficient of some general function, this analysis could help us predict the stable states of such a system. There is a very good possibility that there are many more states, as we haven't comprehensively explored the space defined by the parameters $(K, J, \gamma_1, \gamma_2)$ given its large in size. These new states could provide us with deep insight about the our model, and maybe help formulate a model which would show a new landscape of emergent behavior. One possible area of future research would be to use collective coordinates to reduce high dimensional Swarmalator system, to a few number of active degrees of freedom. This could simplify the dynamics and provide insight about the behavior of rogue swarmalators. One possible real-world swarmalators are biological micro-swimmers, such as spermatoza, which exhibit rich swarming behavior. The phase variable in such sperms could be the rhythmic beating of the sperm's tail.which can synchronize with other sperms. One route to increase more realism would be to study complex coupling parameters as functions of position or phase, or choosing more complicated interaction functions $\mathbf{I}_{att}, \mathbf{I}_{rep}, G, H_{att}$.

All data files used to create plots, run simulations, and GUI will be available at github repository "ankithadas/Extended-Swarmalator-Model".

[1] J. H. Sheeba, A. Stefanovska, and P. V. E. McClintock, "Neuronal synchrony during anesthesia: a thalamocortical model," *Biophysical journal*, vol. 95, no. 18586847, pp. 2722–2727, Sep. 2008. [Online]. Available: https://www.ncbi.nlm.nih.gov/pmc/articles/PMC2527271/

[2] R. E. Mirollo and S. H. Strogatz, "Synchronization of Pulse-Coupled Biological Oscillators," *SIAM Journal on Applied Mathematics*, vol. 50, no. 6, pp. 1645–1662, 1990. [Online]. Available: http://dx.doi.org/10.1137/0150098

[3] G. Filatrella, A. H. Nielsen, and N. F. Pedersen, "Analysis of a power grid using a kuramoto-like model," *The European Physical Journal B*, vol. 61, no. 4, pp. 485–491, Feb. 2008. [Online]. Available: https://doi.org/10.1140/epjb/e2008-00098-8

[4] S. Watanabe and S. H. Strogatz, "Constants of motion for superconducting josephson arrays," *Physica D: Nonlinear Phenomena*, vol. 74, no. 3, pp. 197–253, Jul. 1994. [Online]. Available: http://www.sciencedirect.com/science/article/pii/0167278994901961

[5] Y. Kuramoto, *International Symposium on Mathematical Problems in Theoretical Physics*, 1st ed., H. Araki, Ed. Berlin: Springer-Verlag, 1975, vol. 39.

[6] I. Aihara, H. Kitahata, K. Yoshikawa, and K. Aihara, "Mathematical modeling of frogs' calling behavior and its possible application to artificial life and robotics," *Artificial Life and Robotics*, vol. 12, no. 1, pp. 29–32, Mar. 2008. [Online]. Available: https://doi.org/10.1007/s10015-007-0436-x

[7] E. Montbrió, D. Pazó, and A. Roxin, "Macroscopic description for networks of spiking neurons," *Phys. Rev. X*, vol. 5, p. 021028, Jun 2015. [Online]. Available: https://link.aps.org/doi/10.1103/PhysRevX.5.021028

[8] Z. Néda, E. Ravasz, T. Vicsek, Y. Brechet, and A. L. Barabási, "Physics of the rhythmic applause," *Phys. Rev. E*, vol. 61, pp. 6987–6992, Jun 2000. [Online]. Available: https://link.aps.org/doi/10.1103/PhysRevE.61.6987

[9] K. P. O'Keeffe, H. Hong, and S. H. Strogatz, "Oscillators that sync and swarm," *Nature Communications*, vol. 8, no. 1, p. 1504, Nov. 2017. [Online]. Available: https://doi.org/10.1038/s41467-017-01190-3